

T-Type Ca^{2+} Channels Are Involved in High Glucose-Induced Rat Neonatal Cardiomyocyte Proliferation

MING LI, MIN ZHANG, LUPING HUANG, JIANXIN ZHOU, HEAN ZHUANG, JAMES T. TAYLOR, BRIAN M. KEYSER, AND RICHARD M. WHITEHURST, JR.

Department of Pharmacology [M.L., L.H., J.Z., J.T.T., B.M.K.], Tulane University Health Sciences Center, New Orleans, Louisiana 70112; Department of Pharmacology [M.Z., H.Z., R.M.W.], University of South Alabama College of Medicine, Mobile, Alabama 36688; and Department of Pediatrics [R.M.W.], University of South Alabama College of Medicine, Mobile, Alabama 36688

ABSTRACT

Infants develop hypertrophic cardiomyopathy in ~30% of diabetic pregnancies. We have characterized the effects of glucose on voltage-gated T-type Ca^{2+} channels and intracellular free calcium concentration, $[\text{Ca}^{2+}]_i$, in neonatal rat cardiomyocytes. We found that T-type Ca^{2+} channel current density increased significantly in primary culture neonatal cardiac myocytes that were treated with 25 mM glucose for 48 h when compared with those that were treated with 5 mM glucose. High-glucose treatment also caused a higher Ca^{2+} influx elicited by 50 mM KCl in the myocytes. KCl-induced Ca^{2+} influx was attenuated when nickel was present. Real-time PCR studies demonstrated that mRNA levels of both $\alpha 1\text{G}$ ($\text{Ca}_v3.1$) and $\alpha 1\text{H}$ ($\text{Ca}_v3.2$) T-type Ca^{2+} channels were elevated after high-glucose

treatment. High-glucose also significantly increased ventricular cell proliferation as well as the proportion of cells in the S-phase of the cell cycle; both effects were reversed by nickel or mibefradil. These results indicate that high glucose causes a rise in $[\text{Ca}^{2+}]_i$ in neonatal cardiac myocytes by a mechanism that is associated with the regulation of the T-type Ca^{2+} channel activity. (*Pediatr Res* 57: 550–556, 2005)

Abbreviations

$[\text{Ca}^{2+}]_i$, cytoplasmic free Ca^{2+} concentration
FBS, fetal bovine serum
IDM, infants of diabetic mothers
RT-PCR, reverse transcriptase-PCR

Diabetes is one of the most common medical complications seen in pregnancy. Approximately 3–10% of pregnant women have disorders of glucose intolerance (1). This disease affects the fetal cardiovascular system in many ways, both directly and indirectly. The risk for congenital heart disease in infants of diabetic mothers (IDM) is reported to be 5 times higher than in the general population (2). It has been estimated that 30% of IDM have cardiomegaly, only a few of which develop congestive heart failure (1). Diabetic hypertrophic cardiomyopathy has been associated with poor maternal glucose regulation; however, recent studies indicate that cardiac hypertrophy can be attributed to a more complex mechanism possibly including Ca^{2+} overload (3–5), which may result from an elevated expression of voltage gated Ca^{2+} channels.

Two well-documented voltage gated Ca^{2+} channels found in fetal and neonatal hearts are the L-type and T-type Ca^{2+} channels (6–8). The L-type Ca^{2+} channels become more abundant as some organisms develop into adulthood (8–10); however, T-type Ca^{2+} channels are down-regulated or disappear in adult animals (6,11–14). The density of T-type Ca^{2+} channels is predominant only in pacemaker cells of the sinoatrial node and the Purkinje fibers (15,16). The physiologic role of the T-type Ca^{2+} channel has been postulated to be involved in the cell cycle during proliferation (17); therefore, we expect to see an increase in T-type Ca^{2+} channel activity in glucose-induced neonatal hypertrophic cardiomyopathy secondary to cell proliferation.

We hypothesized that T-type calcium currents would be increased in response to high glucose. We found that this indeed was the case and that many of the effects of high glucose were prevented by manipulations that reduced T-type calcium currents.

METHODS

Cell preparation. Neonatal ventricular myocytes were prepared from the hearts of 4-d-old Charles River rats using a previously described protocol

Received April 20, 2004; accepted September 3, 2004.

Correspondence: Ming Li, Ph.D., Department Pharmacology SL-83, Tulane University Health Sciences Center, 1430 Tulane Avenue, New Orleans, LA 70112; e-mail: mli@tulane.edu.

This study was supported by a research-in-aid award of the American Heart Association to M.L.

DOI: 10.1203/01.PDR.0000155756.89681.3C

(18,19). Briefly, hearts were removed and transferred to a 100-mm dish that contained heparin solution (1× Hanks balanced saline solution, 10 mM HEPES, and 10 units of heparin). After hearts were dissected into two pieces with a surgical scalpel, the tissue was washed once with the heparin solution and incubated with gentle rocking in a solution that contained 1× Hanks balanced saline solution, 10 mM HEPES, and 1 mg/mL trypsin, at 4°C, 75 rpm overnight. The next day, tissue was pipetted five times every 2 min with a 10-mL-wide mouth pipette in a solution that contained 1× Hanks balanced saline solution, 10 mM HEPES, and 1 mg/mL collagenase (Sigma Chemical Co., St. Louis, MO), and the supernatant was discarded at each time. Cardiomyocytes were recovered afterward by resuspending in 10 mL of 10% fetal bovine serum (FBS) in M199 medium. Cells were centrifuged at 1000 rpm for 5 min and washed once with cold M199 medium that contained 10% FBS. Fibroblasts were removed by plating (100-mm dishes) cells at 37°C for 45 min in M199 medium that contained 10% FBS. Cardiomyocytes were recovered by collecting the nonadherent cells and cultured in M199 medium that contained 10% FBS, 10 mM HEPES, 2 mM L-glutamine, 0.2 mg/mL vitamin B₁₂, 100 units/mL penicillin/streptomycin, and 10 mM glutamine. Cells were plated on tissue culture plates that were precoated with 0.1% gelatin at a density of 5 × 10⁵ cells/mL and grown at 37°C in 5% CO₂. Cardiomyocytes were cultured with standard M199 medium that contained 2% FBS, forming a nearly confluent monolayer by the second day after plating. The next day, the cells were changed to a standard serum-free medium plus 56 U/L insulin, and 5 mM glucose or 25 mM glucose, respectively. After a 48- to 72-h incubation period, cells were studied to determine their electrophysiologic and calcium influx properties.

Electrophysiologic recording. The whole-cell recordings were carried out by the standard “giga-seal” patch clamp technique. The whole-cell recording pipettes were made of hemocapillaries (Warner Instrument Corp., Hamden, CT), pulled by a two-stage puller (PC-10; Narishige Int., New York, NY), and heat polished with a microforge (MF-200; World Precision Instruments, Sarasota, FL) before using. The pipette resistance was in the range of 2–5 MΩ with our internal solution. The recordings were performed at room temperature (22°C). Currents were recorded using an EPC-9 patch-clamp amplifier (HEKA, Lambrecht/Pfalz, Germany) and filtered at 2.9 kHz. Data were acquired with Pulse/PulseFit software (HEKA). Voltage-dependent currents were corrected for linear leak and residual capacitance by using an on-line P/4 subtraction. Normalized conductance-voltage relationship curves were fitted with the Boltzmann equation,

$$I + \exp[(V - V_{1/2})/k]$$

where $V_{1/2}$ is the voltage of half activation and k is a slope.

The standard external recording solution contained (in mM) 10 CaCl₂, 110 tetraethylammonium-Cl, 10 CsCl, 10 HEPES, 40 sucrose, and 0.5 3,4-diaminopyridine (pH 7.3). The pipette solution contained (in mM) 130 N-methyl-D-glucamine, 20 EGTA (free acid), 5 bis (2-aminophenoxy) ethane-N, N, N', N'-tetraacetate, 10 HEPES, 6 MgCl₂, and 4 Ca(OH)₂ (pH was adjusted to 7.4 with methanesulfonate). Mg-ATP (2 mM) was included in the pipette solution to minimize rundown of L-type Ca²⁺ currents. In some experiments, a Ba²⁺ external solution was also used (in mM): 40 Ba(OH)₂, 30 tetraethylammonium-OH, 100 sucrose, and 10 HEPES (pH 7.3).

[Ca²⁺]_i measurement using fura-2 fluorescence. Primary cultured myocytes were seeded onto 0.1% gelatin-treated glass coverslips. [Ca²⁺]_i was estimated by using the Ca²⁺-sensitive probe fura-2 AM. The measurement solution contained (in mM) 130 NaCl, 5 KCl, 2 CaCl₂, 1 MgCl₂, and 15 HEPES (pH was adjusted to 7.4 with NaOH). Cells were washed twice before fura-2 AM loading. The depolarizing solution contained (in mM) 85 NaCl, 50 KCl, 2 CaCl₂, 1 MgCl₂, and 15 HEPES, with pH adjusted to 7.4 with NaOH. The loading solution (1 mL) consisted of the measurement solution plus 3 μM fura-2 AM and 3 μL of a 10% Pluronic acid solution. Cells were loaded for 20 min in a 5% CO₂ incubator at 37°C. After this loading period, cells were washed and incubated for de-esterification for 20 min. After de-esterification, [Ca²⁺]_i was assessed with an inverted microscope in conjunction with a Xenon arc lamp photomultiplier system (Ionoptix Inc., Boston, MA). Data were acquired and analyzed with Ionwizard software (Ionoptix). Epifluorescence (signal averaged) was measured from single cells, and the values in [Ca²⁺]_i were determined as the fluorescence ratio (R) of the isobestic point for fura-2 (360 nm) to Ca²⁺-unbound (380 nm) excitation wavelengths emitted at 510 nm.

Reverse transcriptase-PCR. Total RNA was extracted from neonatal cardiac myocytes using the TRIzol reagent method according to the manufacturer's instructions (Life Technologies, Grand Island, NY). First-strand cDNA was made by reverse transcription of 2 μg of total RNA from different treatment groups in 50 μL of reverse transcription buffer that contained 1.5 μM specific primers, 0.5 mM dNTP, 10 μM DTT, 100 U of rRNasin (Promega, Madison, WI), and 500 U of M-MLV reverse transcriptase (Life Technologies) at 37°C for 1 h. The reverse transcriptase was inactivated by

heating at 99°C for 5 min. PCR was carried out in a solution that contained 2× reaction mix (25 μL), SuperScript II RT/Taq Mix (1 μL), RNA (3 μg), and 10 pmol of Ca_v3.1 or Ca_v1.2 forward and reverse primers (Table 1) in a total volume of 50 μL. After incubation at 46°C for 30 min, the mixture was run in a thermocycler for 36 cycles. Each cycle consisted of a denaturing at 94°C for 30 s, annealing at 56°C for 30 s, and extension at 68°C for 1 min, sequentially. After reverse transcriptase-PCR (RT-PCR), 10 μL of each product was loaded onto a 1% agarose gel for electrophoresis.

Quantitative real-time PCR. RNA was extracted using Trizol method, and cDNA synthesis was carried out using the High Capacity cDNA Archive Kit (Applied Biosystems, Foster City, CA) according to the manufacturer's instructions. Before cDNA synthesis, total RNA was treated with DNase I. Two micrograms of total RNA was used in each cDNA synthesis.

Quantitative real-time PCR was performed using SYBR Green PCR Master Mix, and message level was determined using the ΔΔCt method. Quantitative real-time PCR was carried out under the following reaction conditions: stage 1, 50°C for 2 min (rep 1); stage 2, 95°C for 10 min (rep 1); and stage 3, 95°C for 15 s then 60°C for 1 min (reps 40). Ca_v3.1 and Ca_v3.2 primer sequences used in the experiment were designed using Primer Express 1.0 and are shown in Table 2. Experiments were carried out using a Perkin Elmer GeneAmp PCR System 9600 with a GeneAmp 5700 Sequence detector and detection software version 1.3 (Perkin Elmer, Foster City, CA).

Antisense and sense oligonucleotides. T-type Ca²⁺ channel-specific antisense oligonucleotides were designed against the common motif NMFVGV-VVE of DHISVI (20) of Ca_v3.1 (accession no. AF027984) and Ca_v3.2 (accession no. AF290213) and purchased from Sequetur (Natick, MA). Cells were transfected with antisense or sense oligonucleotides by TransFast transfection reagent (Promega). Transfection with oligonucleotides was performed according to the manufacturer's instructions. The oligonucleotides were incubated with TransFast reagent for 15 min at room temperature. Myocytes that were cultured for 24 h were washed to remove serum before addition of oligonucleotides-TransFast mixtures, and incubation was performed for 20 h at 37°C. The TransFast solution was removed, M199 culture medium was added, and the myocytes were cultured at 37°C for 48 h before the experiments.

Protein assay and cell count. Cardiomyocyte cellular protein content was measured by using the standard Bio-Rad protein assay (Bio-Rad Laboratories, Hercules, CA). The cells were counted using the Particle Counter (Coulter Corp., Miami, FL).

Flow cytometry. Rat neonatal ventricular myocytes were cultured in the standard serum-free medium (no insulin) for 48 h. This resulted in >90% of the cardiomyocytes being arrested in the G₀-G₁ phase. After this process, cells were incubated in the same medium as for electrophysiologic studies, supplemented with 5 or 25 mM glucose or 25 mM glucose plus Ca²⁺ channel antagonists for 24 h. Cells then were collected with trypsin-EGTA solution and washed three times with PBS (pH 7.4). Collected cells were resuspended in 1 mL of analysis buffer that contained 0.1% sodium citrate, 0.3% NP-40, 0.05

Table 1. List of the gene-specific primers for RT-PCR

Ca _v 3.1 ^a	Forward	5'-TCATCAGCCGGGCCAGGA-3'
	Reverse	5'-CTTACTCCTTCTCTTTTTC-3'
Ca _v 1.2 ^b	Forward	5'-ATACAAAGACGGAGAAGT-3'
	Reverse	5'-GCTGCATGGCCAGGCAGAT-3'

^a Genbank accession no. AF027984.

^b Genbank accession no. M67515.

Table 2. List of the gene-specific primers for quantitative real-time PCR

Ca _v 3.1 ^a	Forward	5'-CAGACCTGCTGACTGTGAGGAA-3'
	Reverse	5'-CGGCACATGTAGCTGTCATTG-3'
Ca _v 3.2 ^b	Forward	5'-TCCCAACTTTGCCTTTGAG-3'
	Reverse	5'-TGGTCACTGTCCAAGAAACAGTCT-3'
β-actin ^c	Forward	5'-CTTCAACACCCAGCCATGT-3'
	Reverse	5'-GTGGTACGACCAGAGGCATACA-3'

^a Genbank accession no. AF027984.

^b Genbank accession no. AF290213.

^c Genbank accession no. NM031144.

mg/mL propidium iodide, and 0.02 mg/mL RNase. Cells then were stored at 4°C overnight for staining nuclei. Flow cytometry analysis was performed on the FACS Vantage SE (Becton-Dickinson, San Jose, CA), and the data were interpreted using the attached ModFit LT 2.0 cell cycle analysis program. At least 10,000 cells were recorded for each sample.

Statistics. All data are presented as mean \pm SE, and the *t* test was used to calculate *p* values.

RESULTS

To investigate the effects of chronic high glucose concentrations on voltage activated Ca^{2+} currents, we used primary cultured rat neonatal cardiac myocytes that were treated with either 5 or 25 mM glucose for 48 h to evaluate their Ca^{2+} current amplitudes with whole-cell patch clamp. The Ca^{2+} currents were elicited with test pulses stepped between -70 and 40 mV for 100 ms, with 10-mV increments at the membrane holding potential of -80 mV. The amplitudes of the currents were normalized by the membrane capacitances of the corresponding cells. As shown in Fig. 1C, we found that the current densities at -30 mV were -13.6 ± 1.4 pA/pF and -7.5 ± 0.6 pA/pF in cells that were pretreated (48 h) with 25 and 5 mM glucose, respectively. Figure 1A shows the representative traces of currents measured at -30 from cells that were treated with 5 mM (upper) and 25 mM (lower) glucose. The increased current densities were also observed at test potentials between -50 and 0 mV. Because the voltage threshold for T-type Ca^{2+} current activation was ~ -50 mV and the peak current voltage was ~ 0 mV, this suggested that the increases in total Ca^{2+} current were mainly attributed to an increase in low-threshold Ca^{2+} currents, or T-type Ca^{2+} currents. In contrast, the current densities at the voltages positive than 0 mV had fewer differences between the groups that were treated with 5 and 25 mM glucose, indicating that L-type Ca^{2+} currents remained at approximately the same levels. This observation was further confirmed with selectively recording of L-type Ca^{2+} current at 20 mV with holding potential of -40 mV, at which most of the T-type Ca^{2+} currents were inactivated. Figure 1B shows two representative traces of L-type Ca^{2+} current with similar amplitudes from the cells that were treated with 5 mM (upper) or 25 mM (lower) glucose for 48 h, respectively. Increasing the osmotic strength of the normal glucose solution with 20 mM mannitol had no effect on the T-type current density (Fig. 1C).

Chronic high glucose-induced increases in current densities measured at low voltages might also be due to the shift of voltage-dependent activation or inactivation of the T-type Ca^{2+} currents. To examine this possibility, we characterized the voltage-dependent activation and steady-state inactivation of the T-type Ca^{2+} current in the cells that were pretreated with 5 or 25 mM glucose. The voltage-dependent T-type Ca^{2+} conductance was determined by measuring the amplitudes of slow decaying tail currents at -120 mV (200 ms) preceded by a 20-ms testing pulse stepped from -60 mV to 50 mV (10 mV increments). The steady-state inactivation of T-type Ca^{2+} current was determined by measuring the inactivation of the current elicited at -30 mV after 3-s prepulses ranging from -100 to -30 mV. With our external solution that contained 10 mM Ca^{2+} , currents at -30 mV were mainly attributed to T-type Ca^{2+} currents because the currents were completely

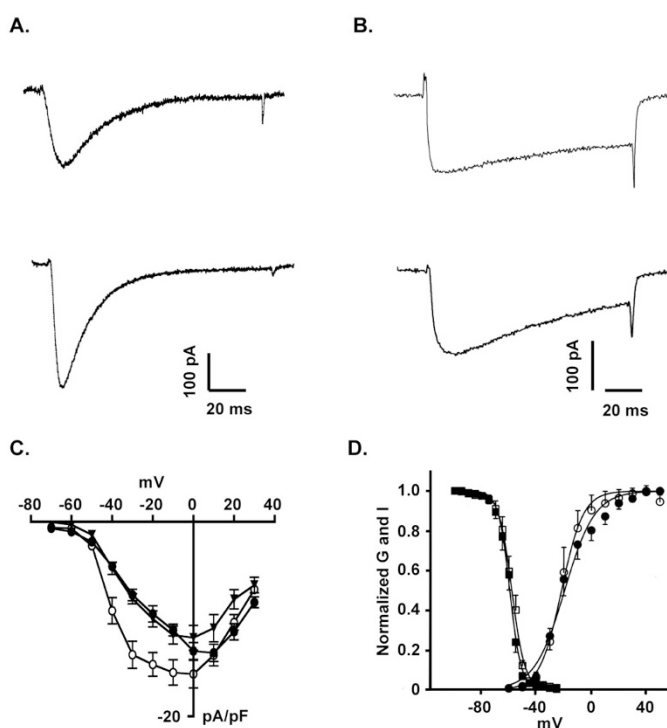


Figure 1. T-type Ca^{2+} current amplitude was elevated by chronic high-glucose treatment. (A) Ca^{2+} currents were elicited by -30 -mV test pulses when held at -80 mV. The upper and lower traces represent currents recorded in cells that were pretreated for 24 h in 5 mM glucose (54.6 pF; control) or 25 mM glucose (47.1 pF; high glucose), respectively. (B) Ca^{2+} currents were elicited by 20-mV test pulses when held at -40 mV (filtered in 1 KHz). The upper and lower traces represent currents recorded in cells that were pretreated for 24 h in 5 or 25 mM glucose, respectively. (C) Relationship between Ca^{2+} current density and voltage (I-V). The holding potential was -80 mV. ●, data from control cells ($n = 20$); ○, data from high glucose-treated cells ($n = 12$); ■, control cells with 20 mM mannitol and 5 mM glucose ($n = 10$). The peak currents measured at the first 50-ms duration of the 200-ms depolarizing pulses. Each point demonstrates mean \pm SEM of the current density. (D) Voltage-dependent activation (G) and steady-state inactivation (I) curves of T-type Ca^{2+} currents from cells that were treated with 5 or 25 mM glucose. The normalized G was plotted as a function of test pulse voltage. The activation data were obtained by measuring the tail current at -100 mV after the stimulation pulses stepped from -60 to 50 mV with a holding potential of -80 mV. The inactivation data were generated with a protocol that consisted of 3-s prepulses ranging from -100 to -25 mV followed immediately by a test pulse (100 ms) to -30 mV. Both activation and inactivation data were normalized to the maximum of the functions and fitted to the Boltzmann equation. Open symbols represent the data from 5 mM glucose-treated cells (con), and closed symbols represent the data from 25 mM glucose-treated cells (glu). [$V_{1/2} = (\text{glu}) -19.4$ mV, (con) -21.7 mV, $k = (\text{glu}) -10.8$, (con) -7.8 , $n = (\text{high glucose}) 8$, (con) 5, for activation curves; $V_{1/2} = (\text{high glucose}) -59.5$ mV, (con) -57.9 mV, $k = (\text{glu}) 4.3$, (con) 4.9, $n = (\text{glu}) 8$, (con) 8, for inactivation curves].

inactivated when a prepulse of -40 mV was applied (Fig. 1D). Data were calculated and fitted with the Boltzmann equation. As shown in Fig. 1D, the T-type Ca^{2+} currents were activated initially at -50 mV and completely inactivated by a prepulse at -40 mV. Pretreating the cells with 25 mM glucose for 48 h did not change the characteristics of either the voltage-dependent activation or steady-state inactivation of T-type Ca^{2+} currents (Fig. 1D).

To selectively block T-type currents in neonatal cardiac myocytes, we examined the effect of a T-type Ca^{2+} channel

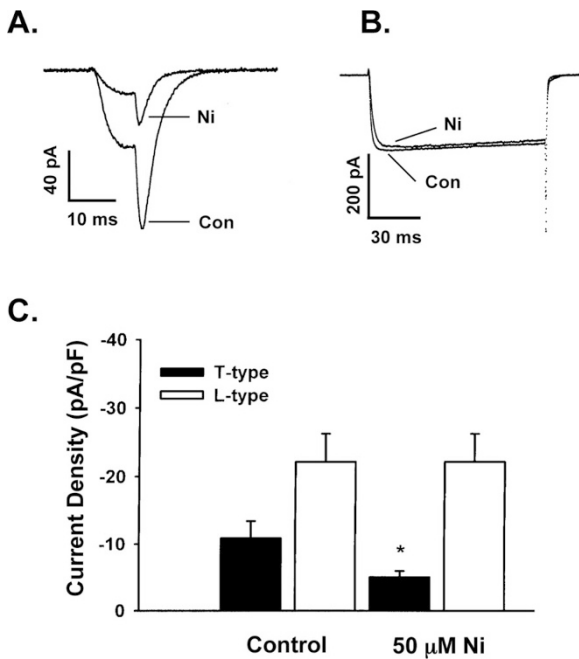


Figure 2. The effect of NiCl_2 ($50 \mu\text{M}$) on the T-type and L-type Ca^{2+} channels in neonatal rat cardiomyocytes using 40 mM BaCl_2 external solution. (A) T-type Ca^{2+} channel tail currents were measured at -100 mV after a 10-ms prepulse at -30 mV with a holding potential of -80 mV . (B) The L-type Ca^{2+} currents were measured before and after NiCl_2 treatment. The currents were elicited by 20-mV test pulses and held at -40 mV (77.3 pF). (C) The average effect of NiCl_2 on the T-type and L-type Ca^{2+} channels. ■, tail-current density ($n = 8$); □, peak current density ($n = 6$). * $p < 0.05$, NiCl_2 vs control.

blocker, nickel ($50 \mu\text{M}$ NiCl_2), on the T- and L-type Ca^{2+} currents in myocytes that were pretreated with 25 mM glucose. In these experiments, T-type Ca^{2+} currents were selectively inhibited by NiCl_2 , which was demonstrated by measuring the slow-decaying tail currents before and after NiCl_2 administration (Fig. 2A). Nickel had no effect on the L-type Ca^{2+} currents that were selectively recorded at a test potential of 20 mV when held at -40 mV with an external solution that contained 40 mM Ba^{2+} (Fig. 2B). Because nickel selectively reduced

T-type Ca^{2+} tail-current density by 51% , whereas its effect on L-type Ca^{2+} current was minimal (Fig. 2C), it suggests that high glucose-treated neonatal myocardial cells expressed more T-type Ca^{2+} currents.

To examine the contribution of increased T-type Ca^{2+} currents in voltage-dependent Ca^{2+} influx, in subsequent experiments conducted in quiescent cardiomyocytes, we used the Ca^{2+} -sensitive fluorescence probe (fura-2 AM) to measure intracellular $[\text{Ca}^{2+}]$ elevation in response to KCl-induced membrane depolarization. High-glucose treatment significantly potentiated the peak amplitude of the intracellular $[\text{Ca}^{2+}]$ elevation elicited by 50 mM KCl as shown in Fig. 3. The Ca^{2+} influxes were reduced when $50 \mu\text{M}$ NiCl_2 was added to the bath solution (Fig. 3C). This result suggested that high-glucose treatment on neonatal myocytes caused an enhanced voltage-dependent Ca^{2+} influx, which may result, at least in part, from the increased expression of T-type Ca^{2+} currents in these cells.

How does chronic high glucose enhance T-type Ca^{2+} channel activity? Are mRNA levels of T-type Ca^{2+} channels regulated by high glucose treatments? If so, is the regulation selective to T-type Ca^{2+} channels? To address these questions, we conducted RT-PCR experiments to evaluate T- and L-type Ca^{2+} channel gene transcriptions under the conditions of 5 and 25 mM glucose treatment in neonatal ventricular myocytes. RT-PCR was carried out with primers for the T-type Ca^{2+} channel isoform, $\text{Ca}_v3.1$ (21), and an L-type Ca^{2+} channel isoform, $\text{Ca}_v1.2$. Each RT-PCR product was sequenced and matched to known sequences. The result indicated that 25 mM glucose induced an increase in mRNA level of the $\text{Ca}_v3.1$ channel after $1, 6, 12,$ and 24 h of treatment when compared with the paired 5-mM glucose incubation groups (Fig. 4A). In contrast, no significant difference in mRNA levels of the $\text{Ca}_v1.2$ was observed between the low glucose- and high glucose-treated groups for $2, 12,$ and 34 h (Fig. 4B). Similar results were obtained from three repeated experiments. These results indicated that a high concentration of glucose up-regulated T-type Ca^{2+} channel but not L-type Ca^{2+} channel mRNA expression in rat neonatal cardiomyocytes.

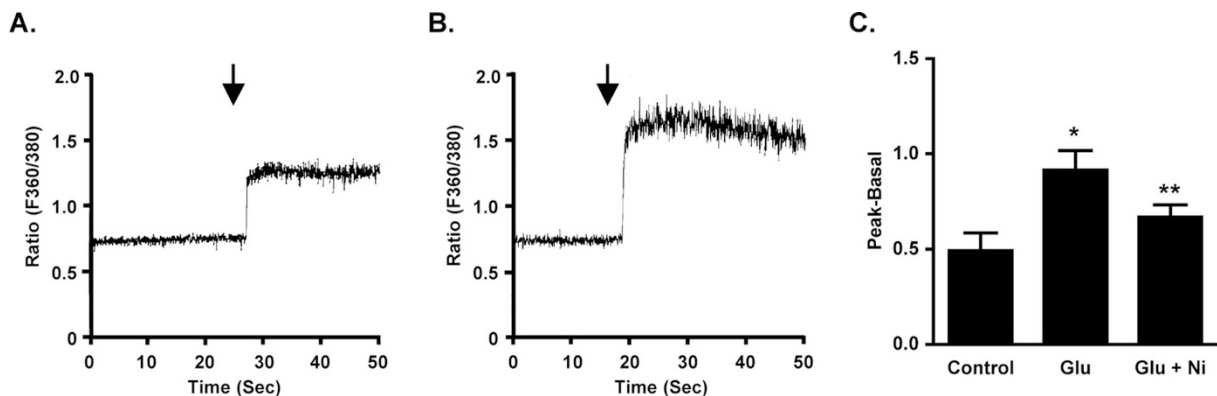


Figure 3. Ca^{2+} influx measured by fura-2 fluorescence ratio with excitation UV light at $360/380 \text{ nm}$ in neonatal rat cardiomyocytes. Data were sampled every 50 ms . Representative traces were recorded from cells that were pretreated with 5 mM glucose (control; A) or 25 mM glucose (high glucose; B) for 48 h . Arrows indicate the time when 50 mM KCl was perfused into the recording chamber. (C) Peak ratio-basal ratio represents the average increments of the KCl-induced $[\text{Ca}^{2+}]$ elevation, which was calculated by subtracting the average fluorescent ratio ($360/380 \text{ nm}$) values before KCl perfusion (basal) from the highest value after KCl perfusion (peak) of each stimulation. The average ratios and SEs were obtained from control cells ($n = 11$), high glucose-treated cells ($n = 9$), and high glucose plus $50 \mu\text{M}$ NiCl_2 -treated cells ($n = 9$). *High glucose vs control ($p < 0.05$); **high glucose plus NiCl_2 vs high glucose ($p < 0.05$).

We also used real-time PCR technology to quantitatively measure the level of high glucose–regulated $Ca_v3.1$ and $Ca_v3.2$ (22) mRNA expression. When neonatal cardiomyocytes were treated with 25 mM glucose for 1, 6, 12, 24, and 48 h, we found larger increases of mRNA levels of T-type Ca^{2+} channels at early time points (1 and 6 h) and a smaller but sustained elevation of both mRNA levels for longer time points (Fig. 4C).

Because high-concentration glucose increases T-type Ca^{2+} channel current expression and voltage-dependent Ca^{2+} influx, it is important to learn the role of these channels in neonatal

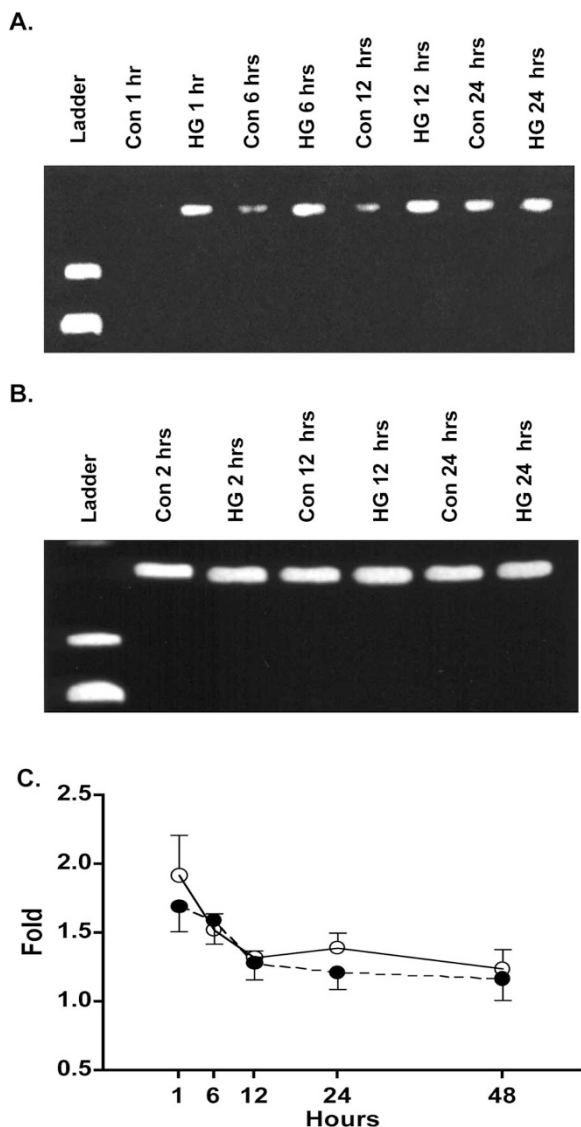


Figure 4. Evaluation of the effect of chronic high-glucose treatment on the mRNA expression of $Ca_v1.2$, $Ca_v3.1$, and $Ca_v3.2$ subunits in neonatal rat cardiomyocyte with RT-PCR and quantitative real-time PCR method. (A) RT-PCR yielded a 479-bp fragment of $Ca_v3.1$. Control groups were treated with 5 mM glucose, and high glucose groups were treated with 25 mM glucose. (B) RT-PCR yielded a 494-bp fragment of $Ca_v1.2$. Control groups were treated with 5 mM glucose and high glucose groups were treated with 25 mM glucose. (C) The $Ca_v3.1$ and $Ca_v3.2$ mRNA levels were expressed as fold increase in 25 mM glucose treatment over the control (5 mM glucose) at various times. ○, value of $Ca_v3.1$ subunit; ●, value of $Ca_v3.2$ subunits. Error bars represent the standard errors; $n = 6$ for both groups.

cardiomyocyte proliferation. We used antisense and sense oligonucleotides against both $Ca_v3.1$ and $Ca_v3.2$ T-type Ca^{2+} channels to selectively inhibit the function of T-type Ca^{2+} channels. The inhibitory effect of the antisense oligonucleotides on T-type Ca^{2+} currents has been confirmed in neurons previously (20). We further tested the effects of these oligonucleotides on T- and L-type Ca^{2+} channel activities, respectively. Current densities in the cells that were treated with sense or antisense oligonucleotides for 48 h were recorded with voltage protocols that were selective to T- or L-type channels. Figure 5A shows that the current density measured at -30 mV with holding potential of -80 mV, which predominantly records T-type Ca^{2+} currents, was significantly suppressed in the $Ca_v3.1/Ca_v3.2$ antisense oligonucleotide–treated cells when compared with the cells that were treated with the sense oligonucleotides. In contrast, no significant difference was observed in these cells when the current densities were measured at 20 mV with holding potential of -40 mV, which exclusively records L-type Ca^{2+} currents (Fig. 5B). These results suggest that the antisense oligonucleotides selectively and effectively reduced T-type Ca^{2+} channel currents in neonatal cardiomyocytes. Cellular proliferation was monitored by measuring [3 H]thymidine incorporation in rat neonatal cardiomyocytes. The cells were transfected with either antisense or sense oligonucleotides for 48 h. At the last 4 h, 2 μ Ci of [3 H]thymidine was added into the culture medium. We found that the antisense oligonucleotides suppressed [3 H]thymidine incorporation significantly when compared with that transfected with sense oligonucleotides (Fig. 5C). These data suggest that T-type Ca^{2+} channels play an important role in rat neonatal cardiomyocyte proliferation.

To reveal the mechanism by which T-type Ca^{2+} channels affect neonatal cardiomyocyte proliferation, we investigated the pharmacologic effect of T-type Ca^{2+} channel antagonists on the phase distribution of the cell cycles. Flow cytometric technique was used to determine the proportion of cells in different phases of the cell cycle. High-glucose (25 mM) treatment profoundly increased the percentage of cells in the S phase as seen in Fig. 6, whereas the presence of 50 μ M $NiCl_2$ or 1 μ M mibefradil, another Ca^{2+} channel antagonist (23), effectively reversed this effect. In contrast to high glucose alone, the L-type Ca^{2+} channel antagonist nifedipine (10 μ M) did not have a significant effect on the proportion of cells in S-phase. These results suggested that high glucose caused an increase in DNA synthesis in cultured rat neonatal ventricular myocytes and that T-type Ca^{2+} channels play an important role before or during the S-phase of mitosis.

Is increased expression of T-type Ca^{2+} currents and correspondingly increased Ca^{2+} influx involved with high glucose–induced hyperplasia? We addressed this question by examining the effect of nickel on the total number of cells and total protein content of cells that were treated with high glucose. We found that 25-mM glucose treatment substantially increased cell number until the culture was confluent. This effect was reversed when 50 μ M nickel was included in the growth medium (Fig. 7A). However, high-glucose treatment did not affect total protein content (Fig. 7B). This result indicated that high concentration of glucose promoted an increase in rat neonatal

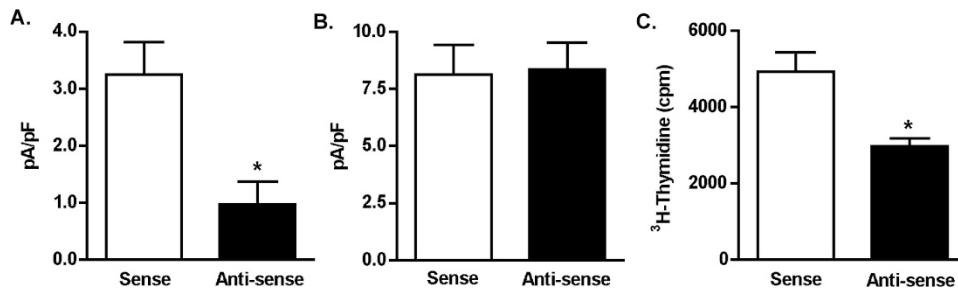


Figure 5. Effects of antisense oligonucleotides against the common motif of the $Ca_v3.1$ and $Ca_v3.2$ subunits of T-type Ca^{2+} channels on cardiomyocyte Ca^{2+} currents and cell proliferation. (A) Ca^{2+} current densities measured at -30 mV when held at -80 mV; $n = 8$; $*p < 0.05$. (B) Ca^{2+} current densities measured at 20 mV when held at -40 mV; $n = 8$; $*p < 0.05$. (C) $[^3H]$ thymidine incorporation in the cardiomyocytes that were transfected with antisense or sense oligonucleotides of T-type Ca^{2+} channel; $n = 4$; $*p < 0.05$.

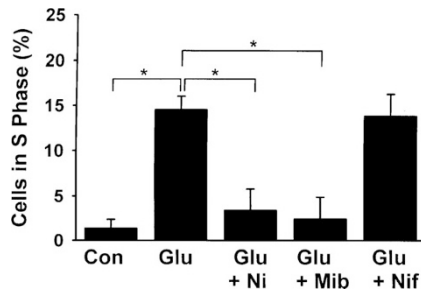


Figure 6. Flow cytometric analysis of cell-cycle distribution. Isolated neonatal cardiomyocytes were incubated for 48 h in serum-free solution supplemented with or without 25 mM glucose (Glu), 50 μ M $NiCl_2$ (Ni) or 1 μ M mibefradil (Mib), or 10 μ M nifedipine. Fraction of cells in S phase was analyzed by FACS after the incubation. Results are expressed as mean \pm SD ($n = 3$). *Significant differences between marked groups by *t* test ($p < 0.05$).

cardiomyocyte proliferation but not cell hypertrophy *via* a T-type Ca^{2+} channel activity-dependent mechanism.

The notion that lack of hypertrophic effect of high-glucose treatments is also supported by the capacitance measurement of individual cells that underwent whole-cell recording, because the membrane capacitance is proportional to the surface area of the cells. We found no significant difference in the membrane capacitances between the low glucose- (26.6 ± 3.9 pF, $n = 44$) and high glucose-treated groups (30.1 ± 6.7 pF, $n = 21$; $p > 0.5$). This supported the hyperplasia not the hypertrophy mechanism.

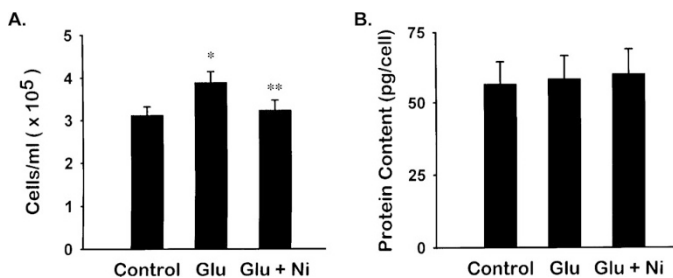


Figure 7. Effects of 25 mM glucose and 50 μ M $NiCl_2$ on the total cell number ($n = 16$; A) and total protein contents of neonatal rat cardiomyocytes ($n = 8$; B) determined at 72 h of high glucose culture. There is a significant increase in cell number ($*p < 0.05$) but not in protein content in the 25 mM glucose-treated cells (Glu). Addition of $NiCl_2$ to the high-glucose group (Glu + Ni) significantly reduced cell number ($**p < 0.05$).

DISCUSSION

It has been reported that T-type Ca^{2+} channels were up-regulated in an experimental model of cardiac hypertrophy and were involved in myocardial remodeling (24). In the heart, T-type Ca^{2+} channels can be induced by angiotensin II (25) or endothelin-1 (26); here, we report that high concentration of glucose might also induce the messenger level of these channels in rat neonatal cardiomyocytes.

The purpose of this study was to investigate the pathophysiologic role of T-type Ca^{2+} channels in high glucose-induced myocardial hypertrophy in neonatal rat heart. Because T-type Ca^{2+} channel current is more prevalent during the embryonic, fetal, and neonatal periods and disappears during maturation into adulthood, it has been postulated that the T-type Ca^{2+} channel is important in the maturation/differentiation process. In primary cultured rat aortic smooth muscle cells, a T-type Ca^{2+} current was present in cells during the G_1 and S phase but decreased or was absent in all other phases of cell division (27). It was shown that cultured smooth muscle cells had an increased T-type Ca^{2+} current during proliferation, and this current decreased as the cells became confluent or when they came in contact with each other (28). In our study, T-type Ca^{2+} current density was significantly greater in high glucose-treated cells compared with controls, which indicated that these channels might play an important role in proliferation, particularly in the S phase of cell cycle in cardiomyocytes.

Transient increases in $[Ca^{2+}]_i$ has been reported to be essential in the progression through specific stages of the cell cycle in different mammalian cells (29). The machinery underlying calcium effects may involve many intracellular signal pathways, such as G protein, protein kinase C, calmodulin, m-calpain, mitogen-activated protein kinase, cyclin-dependent kinase 2, phosphatases, and others (30–33). In addition, Ca^{2+} influx may directly or indirectly alter the plasma membrane potential, which is a critical factor for cell cycling (34). T-type Ca^{2+} currents may contribute to the modulation of calcium homeostasis in these cells. Our results suggest that high glucose induced an overexpression of T-type Ca^{2+} channels, which increases the proliferation rate of neonatal cardiomyocytes.

IDM have a higher rate of congenital anomalies than the general population. Many IDM have a thickened interventricular septum and wall. The most frequent defects are congenital

heart diseases, including hypertrophic cardiomyopathy (35), which has been linked to gestational diabetes of the women (36). In this study, we report data supporting the concept that these defects are directly correlated to poor maternal metabolic control. More specific, the regulation of T-type Ca^{2+} channels by high glucose reported in this study may represent an important pathologic process of hypertrophic cardiomyopathy seen in IDM. Our results suggest that control of plasma glucose concentration in diabetic mothers may play an effective role in prevention or treatment of these cardiac abnormalities in IDM.

Nickel has been shown previously to have toxic effects on cells after a 24-h incubation period with concentrations higher than 100 μM (37). We have previously shown that high concentrations (100 μM or more) of nickel also block L-type Ca^{2+} channels (38); for these reasons, we chose to use a relatively low concentration (50 μM) of nickel in our experiments. It has been shown that the T-type Ca^{2+} currents in the cardiomyocytes of rat and guinea pig are sensitively blocked by nickel at a similar concentration (40 μM) to that used in our study (39,40). It is known that $\text{Ca}_v3.2$ is highly sensitive to nickel (41). The nickel effect seen in our and others' studies using cardiomyocytes might be mainly attributed to its effect on the $\text{Ca}_v3.2$ Ca^{2+} channel, which plays an important role in the cardiomyocyte function. However, the role of $\text{Ca}_v3.1$ might also be considered because it has been shown that a $\text{Ca}_v3.1$ splicing isoform ($\text{Ca}_v3.1d$) expressed in the developing heart can be half blocked by 100 μM NiCl_2 (42). Our data show that T-type Ca^{2+} channels contribute significantly to the cardiomyocyte proliferation.

REFERENCES

- Moore TR 1999 Maternal-Fetal Medicine, 4th Ed. W.B. Saunders Co, Philadelphia, pp 964–995
- Ayres NA 1998 Fetal Cardiology, 2nd Ed. Williams & Wilkins, Baltimore, pp 2281–2300
- Haase H, Kresse A, Hohaus A, Schulte HD, Maier M, Osterziel KJ, Lange PE, Morano I 1996 Expression of calcium channel subunits in the normal and diseased human myocardium. *J Mol Med* 74:99–104
- Nuss HB, Houser SR 1993 T-type Ca^{2+} current is expressed in hypertrophied adult feline left ventricular myocytes. *Circ Res* 73:777–782
- Schaffer SW, Mozaffari MS, Artman M, Wilson GL 1989 Basis for myocardial mechanical defects associated with non-insulin-dependent diabetes. *Am J Physiol* 256:E25–E30
- Gomez JP, Potreau D, Branka JE, Raymond G 1994 Developmental changes in Ca^{2+} currents from newborn rat cardiomyocytes in primary culture. *Pflügers Arch* 428:241–249
- Nalivaiko E, Pronchuk N, Sagach V 1992 Changes in T-type and L-type calcium current densities in newborn rat cardiomyocytes in culture. *J Physiol* 446:145P
- Wang R, Karpinski E, Pang PK 1991 Two types of voltage-dependent calcium channel currents and their modulation by parathyroid hormone in neonatal rat ventricular cells. *J Cardiovasc Pharmacol* 17:990–998
- Kazazoglou T, Schmid A, Renaud JF, Lazdunski M 1983 Ontogenic appearance of Ca^{2+} channels characterized as binding sites for nitrendipine during development of nervous, skeletal and cardiac muscle systems in the rat. *FEBS Lett* 164:75–79
- Wibo M, Bravo G, Godfraind T 1991 Postnatal maturation of excitation-contraction coupling in rat ventricle in relation to the subcellular localization and surface density of 1,4-dihydropyridine and ryanodine receptors. *Circ Res* 68:662–673
- Beam KG, Knudson CM 1988 Effect of postnatal development on calcium currents and slow charge movement in mammalian skeletal muscle. *J Gen Physiol* 91:799–815
- Bkaily G, Sculptoreanu A, Jacques D, Economos D, Menard D 1992 Apamin, a highly potent fetal L-type Ca^{2+} current blocker in single heart cells. *Am J Physiol* 262:H463–H471
- Richard S, Neveu D, Carnac G, Bodin P, Travo P, Nargeot J 1992 Differential expression of voltage-gated Ca^{2+} -currents in cultivated aortic myocytes. *Biochim Biophys Acta* 1160:95–104
- Sen L, Smith TW 1994 T-type Ca^{2+} channels are abnormal in genetically determined cardiomyopathic hamster hearts. *Circ Res* 75:149–155
- Bean BP 1989 Classes of calcium channels in vertebrate cells. *Annu Rev Physiol* 51:367–384
- Katz AM 1996 Calcium channel diversity in the cardiovascular system. *J Am Coll Cardiol* 28:522–529
- Guo W, Kamiya K, Kodmam I, Toyama J 1998 Cell cycle-related changes in the voltage-gated Ca^{2+} currents in cultured newborn rat ventricular myocytes. *J Mol Cell Cardiol* 30:1095–1103
- Simpson P, Savion S 1982 Differentiation of rat myocytes in single cell cultures with and without proliferating nonmyocardial cells. Cross-striations, ultrastructure, and chronotropic response to isoproterenol. *Circ Res* 50:101–116
- Long CS, Henrich CJ, Simpson PC 1991 A growth factor for cardiac myocytes is produced by cardiac nonmyocytes. *Cell Regul* 2:1081–1095
- Lambert RC, McKenna F, Maulet Y, Talley EM, Bayliss DA, Cribbs LL, Lee JH, Perez-Reyes E, Feltz A 1998 Low-voltage-activated Ca^{2+} currents are generated by members of the Ca_vT subunit family ($\alpha_1\text{G}/\text{H}$) in rat primary sensory neurons. *J Neurosci* 18:8605–8613
- Zhuang H, Bhattacharjee A, Hu F, Zhang M, Goswami T, Wang L, Wu S, Berggren PO, Li M 2000 Cloning of a T-type Ca^{2+} channel isoform in insulin-secreting cells. *Diabetes* 49:59–64
- Cribbs LL, Lee JH, Yang J, Satin J, Zhang Y, Daud A, Barclay J, Williamson MP, Fox M, Rees M, Perez-Reyes E 1998 Cloning and characterization of α1H from human heart, a member of the T-type Ca^{2+} channel gene family. *Circ Res* 83:103–109
- Mishra SK, Hermsmeyer K 1994 Selective inhibition of T-type Ca^{2+} channels by Ro 40–5967. *Circ Res* 75:144–148
- Clozel JP, Ertel EA, Ertel SI 1999 Voltage-gated T-type Ca^{2+} channels and heart failure. *Proc Assoc Am Physicians* 111:429–437
- Ferron L, Capuano V, Ruchon Y, Deroubaix E, Coulombe A, Renaud JF 2003 Angiotensin II signaling pathways mediate expression of cardiac T-type calcium channels. *Circ Res* 93:1241–1248
- Izumi T, Kihara Y, Sarai N, Yoneda T, Iwanaga Y, Inagaki K, Onozawa Y, Takenaka H, Kita T, Noma A 2003 Reinduction of T-type calcium channels by endothelin-1 in failing hearts in vivo and in adult rat ventricular myocytes in vitro. *Circulation* 108:2530–2535
- Kuga T, Kobayashi S, Hirakawa Y, Kanaide H, Takeshita A 1996 Cell cycle-dependent expression of L- and T-type Ca^{2+} currents in rat aortic smooth muscle cells in primary culture. *Circ Res* 79:14–19
- Richard S, Tiaho F, Charnet P, Nargeot J, Nerbonne JM 1990 Two pathways for Ca^{2+} channel gating differentially modulated by physiological stimuli. *Am J Physiol* 258:H1872–H1881
- Ciapa B, Pesando D, Wilding M, Whitaker M 1994 Cell-cycle calcium transients driven by cyclic changes in inositol trisphosphate levels. *Nature* 368:875–878
- Ariyoshi H, Okahara K, Sakon M, Kambayashi J, Kawashima S, Kawasaki T, Monden M 1998 Possible involvement of m-calpain in vascular smooth muscle cell proliferation. *Arterioscler Thromb Vasc Biol* 18:493–498
- Akagi K, Nagao T, Urushidani T 1999 Correlation between Ca^{2+} oscillation and cell proliferation via CCK(B)/gastrin receptor. *Biochim Biophys Acta* 1452:243–253
- Chen YJ, Lin JK, Lin-Shiau SY 1999 Proliferation arrest and induction of CDK inhibitors p21 and p27 by depleting the calcium store in cultured C6 glioma cells. *Eur J Cell Biol* 78:824–831
- Baral E, Nagy E, Kwok S, McNicol A, Gerrard J, Berczi I 2000 Suppression of lymphocyte mitogenesis by tamoxifen: studies on protein kinase C, calmodulin and calcium. *Neuroimmunomodulation* 7:68–76
- Wonderlin WF, Strobl JS 1996 Potassium channels, proliferation and G_1 progression. *J Membr Biol* 154:91–107
- Tyralla EE 1996 The infant of the diabetic mother. *Obstet Gynecol Clin North Am* 23:221–241
- Mehta S, Nuamah I, Kalhan S 1991 Altered diastolic function in asymptomatic infants of mothers with gestational diabetes. *Diabetes* 40(suppl 2):56–60
- Repetto G, del Peso A, Sanz P, Repetto M 2001 In vitro effects of lithium and nickel at different levels on Neuro-2a mouse Neuroblastoma cells. *Toxicol In Vitro* 15:363–368
- Bhattacharjee A, Whitehurst RM Jr, Zhang M, Wang L, Li M 1997 T-type Calcium channels facilitate insulin secretion by enhancing general excitability in the insulin-secreting β -cell line, INS-1. *Endocrinology* 138:3735–3740
- Nair RR, Nair P 2001 Age-dependent variation in contractility of adult myocytes. *Int J Biochem Cell Biol* 33:119–125
- Pascarel C, Brette F, Le Guennec JY 2001 Enhancement of the T-type calcium current by hypotonic shock in isolated guinea-pig ventricular myocytes. *J Mol Cell Cardiol* 33:1363–1369
- Lee JH, Gomora J, Cribbs LL, Perez-Reyes E 1999 Nickel block of three cloned T-type calcium channels: low concentrations selectively block α1H . *Biophys J* 77:3034–3042
- Cribbs LL, Martin BL, Schroder EA, Keller BB, Delisle BP, Satin J 2001 Identification of the T-type calcium channel ($\text{Ca}_v3.1d$) in developing mouse heart. *Circ Res* 88:403–407